

Revealing Topological Organization of Human Brain Functional Networks with Resting-State Functional near Infrared Spectroscopy

Haijing Niu¹, Jinhui Wang¹, Tengda Zhao, Ni Shu, Yong He*

State Key Laboratory of Cognitive Neuroscience and Learning, Beijing Normal University, Beijing, People's Republic of China

Abstract

Background: The human brain is a highly complex system that can be represented as a structurally interconnected and functionally synchronized network, which assures both the segregation and integration of information processing. Recent studies have demonstrated that a variety of neuroimaging and neurophysiological techniques such as functional magnetic resonance imaging (fMRI), diffusion MRI and electroencephalography/magnetoencephalography can be employed to explore the topological organization of human brain networks. However, little is known about whether functional near infrared spectroscopy (fNIRS), a relatively new optical imaging technology, can be used to map functional connectome of the human brain and reveal meaningful and reproducible topological characteristics.

Results: We utilized resting-state fNIRS (R-fNIRS) to investigate the topological organization of human brain functional networks in 15 healthy adults. Brain networks were constructed by thresholding the temporal correlation matrices of 46 channels and analyzed using graph-theory approaches. We found that the functional brain network derived from R-fNIRS data had efficient small-world properties, significant hierarchical modular structure and highly connected hubs. These results were highly reproducible both across participants and over time and were consistent with previous findings based on other functional imaging techniques.

Conclusions: Our results confirmed the feasibility and validity of using graph-theory approaches in conjunction with optical imaging techniques to explore the topological organization of human brain networks. These results may expand a methodological framework for utilizing fNIRS to study functional network changes that occur in association with development, aging and neurological and psychiatric disorders.

Citation: Niu H, Wang J, Zhao T, Shu N, He Y (2012) Revealing Topological Organization of Human Brain Functional Networks with Resting-State Functional near Infrared Spectroscopy. PLoS ONE 7(9): e45771. doi:10.1371/journal.pone.0045771

Editor: Satoru Hayasaka, Wake Forest School of Medicine, United States of America

Received: February 24, 2012; **Accepted:** August 22, 2012; **Published:** September 24, 2012

Copyright: © 2012 Niu et al. This is an open-access article distributed under the terms of the Creative Commons Attribution License, which permits unrestricted use, distribution, and reproduction in any medium, provided the original author and source are credited.

Funding: This work was supported by the Natural Science Foundation of China (grant numbers 81030028 and 81201122). The funders had no role in study design, data collection and analysis, decision to publish, or preparation of the manuscript.

Competing Interests: The authors have declared that no competing interests exist.

* E-mail: yong.he@bnu.edu.cn

¹ These authors contributed equally to this work.

Introduction

The human brain is a highly complex network that is interconnected structurally by a dense of cortico-cortical axonal pathways [1] and functionally through synchronized or coherent neural activity [2]. Mapping the human connectome and highlighting its underlying organizational principles are crucial to understanding the architecture of the brain and revealing connectivity changes in entire assemblages of the brain that occur in response to neurological and psychiatric disorders.

Recent studies have shown that human brain networks can be constructed from a variety of neuroimaging and neurophysiological techniques (e.g., structural MRI, diffusion MRI, functional MRI and electroencephalography/magnetoencephalography) and further quantitatively analyzed with graph-theory methods. Graph-based network analysis approaches are straightforward but powerful in characterizing topological properties of the brain networks. Using this theory, it has been shown that human brain

networks possess many non-trivial topological properties such as small-world topology, modularity and highly connected hubs [3–6]. Moreover, these properties exhibit specific alterations during normal development, aging or under pathological conditions [7–11]. Although several imaging techniques have been employed extensively to study connectivity patterns in the brain, it is still largely unknown whether functional near infrared spectroscopy (fNIRS), a relatively new optical imaging technology, can be used to map the functional connectome of the human brain and reveal its underlying infrastructure.

The fNIRS technique uses light in the near-infrared spectrum (670–900 nm) to noninvasively monitor hemodynamic responses evoked by brain activity and to obtain quantitative concentration changes in two chromophores of oxygenated hemoglobin (oxy-Hb) and deoxygenated hemoglobin (deoxy-Hb) in blood flow [12,13]. Relative to functional MRI (fMRI), fNIRS has several advantages such as portability, a lower cost, and a higher temporal sampling rate (≥ 10 Hz). It is also more convenient for studying special

populations (e.g., infants and patients with severe movement disorders). To date, fNIRS has been increasingly used not only to localize focal brain activation during cognitive engagement [14–19], but also to map the functional connectivity of spontaneous brain activity during resting state [20–23]. The resting state is a natural condition in which there is neither overt perceptual input nor behavioral output. Due to its convenience and comparability across different studies and its reflection of spontaneous brain activity, the resting state is becoming a vital experimental paradigm to study brain function [24,25]. There are currently two strategies for deriving resting-state functional connectivity from fNIRS data: one is a seed-based correlation approach that computes temporal correlations between a pre-defined channel of interest and other channels, and the other is independent component analysis (ICA) which utilizes the whole dataset (i.e., all channels) to divide the brain into several statistically independent functional systems (i.e., components). Using these two approaches, several studies have demonstrated strong functional connectivity between bilateral sensorimotor, auditory and visual systems in adults [20–22] and connectivity changes during the normal development of early infancy [26] and in neurological disorders [27]. Importantly, the resting-state functional connectivity revealed by fNIRS has also been proven to be test-retest reliable at both individual and group levels [28] and reproducible among various imaging systems [29]. **Therefore, these studies have provided evidence that fNIRS has the power to detect the functional connectivity of the brain. However, it should be noted that the current fNIRS analysis methods (e.g., seed- or ICA-based functional connectivity) can only be used to reveal single functional connections or connectivity components of the brain. They cannot uncover organizational principles governing these connectivity patterns.**

In this study, we aim to use resting-state fNIRS (R-fNIRS) and graph-theory methods to investigate the topological architecture of functional connectivity patterns in the human brain. The motivation of the current study is that if R-fNIRS can be used successfully to map brain connectome and reveal reproducible and meaningful topological architecture, it will not only broaden our understanding of functional brain connectome but also expand methodological framework for current connectome studies. This is extremely attractive given several unique advantages of fNIRS, such as high temporal resolution and insensitivity to subject motion, which enable researchers to exploit dynamically instantaneous changes of functional brain connectome and special populations (e.g., neonates). To this end, we collected R-fNIRS data of 15 healthy young adults and then constructed brain functional networks by computing correlation matrices between the time series of 46 measurement channels for each participant. The resulting correlation matrices were then averaged to obtain a population-based connectivity backbone network. Finally, we calculated several topological parameters (e.g., small-world, efficiency, module and network hubs) of the group-level brain network as a function of connectivity thresholds and further examined the reproducibility of our findings. This allows us to utilize R-fNIRS data and graph-theory methods to systematically investigate the topological organization of human brain functional networks.

Materials and Methods

Participants and Protocol

Participants included 21 healthy young adults who were between 18 and 26 years of age (15 male, mean age 23.5 years). During R-fNIRS data collection, the participants were instructed

to remain still and keep their eyes closed without falling asleep. For each participant, the data collection lasted 10 minutes. We excluded data from 6 participants because of large motion artifacts in the signals due to head movements or because of failure in probe placement due to obstruction by hair (see Data preprocessing). Thus, only data from 15 participants (10 male, mean age 22.3 years) were included in the final analysis. All participants provided written informed consent, and this study was approved by the Institutional Review Board of the State Key Laboratory of Cognitive Neuroscience and Learning at Beijing Normal University.

Data Acquisition

A continuous wave (CW), near-infrared diffuse optical tomography instrument (CW6, TechEn Inc., MA, USA) was used for data acquisition. The instrument generated two wavelengths of near-infrared light (690 and 830 nm) and measured the time courses of changes in oxyhemoglobin (oxy-Hb) and deoxyhemoglobin (deoxy-Hb) for multiple channels based on the modified Beer-Lambert law [30]. The instrument consisted of 12 laser sources (each with two wavelengths) and 24 detectors. During the experiment, these sources and detectors were systematically embedded in a soft plastic holder that was then secured to the participant's head with Velcro straps. Each adjacent source-detector pair defined a single measurement channel, to be set at 3.2 cm on the spatial separation. This design allowed for 46 different measurement channels, and guaranteed that almost the whole head, including frontal, temporal, parietal and occipital lobes of each hemisphere would be covered (Fig. 1A). The positioning of the probe array was determined according to the international 10–20 system of electrode placement and referred to the external auditory canals and vertex of each participant as landmarks. Specifically, the detectors below channels 17 to 24 in both hemispheres were set along a coronal line from the vertex to the external auditory pores, thus their midline was localized in Cz and the leftmost and rightmost detectors were fitted around T3 and T4, respectively. The position of the array relative to the landmarks was measured to establish repeatable positioning.

Data Preprocessing

We excluded the data that included motion artifacts by examining visually sharp changes in the time series of hemoglobin concentration [27,31–33]. We also used visual inspection to remove data that contained low signal-to-noise ratio at one or several channel(s) due to failures in source/detector placement [21]. With these strict criteria, we ultimately selected 15 participants' data for further analysis.

For each individual's R-fNIRS data, we visually inspected all the R-fNIRS time courses and found that there were unstable signals in some initial time points of the R-fNIRS scan for several participants, which could be attributable to the inadaptation of the subjects to the scanning environments and/or the unachieved stationary state of the scanning equipment. To obtain relatively steady signals and rule out the potential effects of unstable signals on subsequent functional connectivity and network topology analyses, we discarded the first 2 min data for each participant. The critical 2 min time point was chosen to ensure the steady of all time courses from each channel and participant. This procedure is employed in previous fNIRS studies [34–36]. We then digitally band-pass filtered (0.009 – 0.08 Hz) the raw optical density data to reduce the effects of low-frequency drift and high-frequency neurophysiological noise [22,37]. Based on the filtered data from the two wavelengths (690 and 830 nm), we calculated the relative changes in the concentrations of oxy-Hb and deoxy-Hb with the

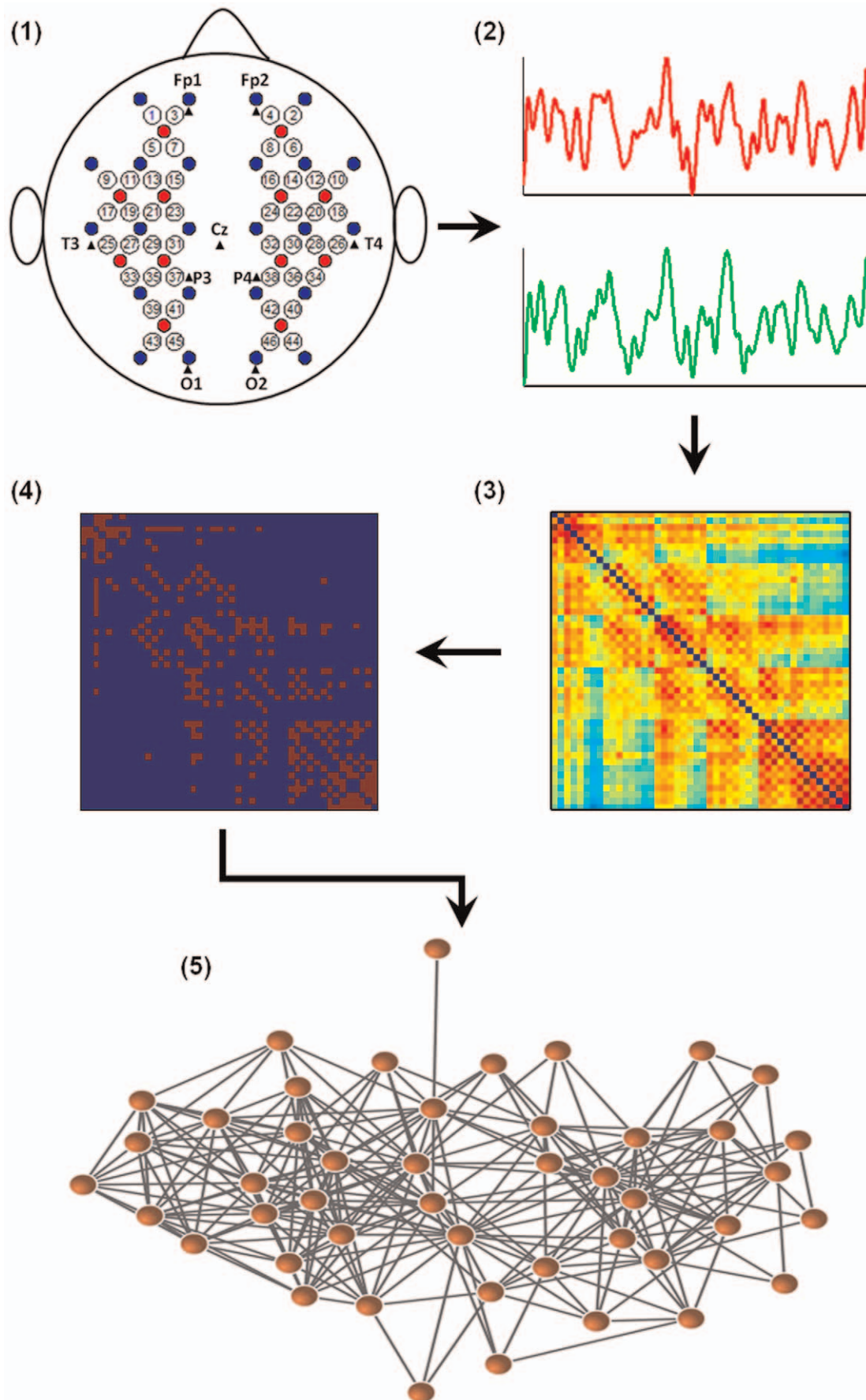


Figure 1. Flowchart for the construction of a functional brain network using R-fNIRS data. (1) Schematic arrangement of the probe array (12 sources, red, and 24 detectors, blue, which configurate 46 measurement channels over the whole head, as indicated by digits from 1 to 46). (2) Extraction of the time course from R-fNIRS data from each measurement channel (i.e., network node). (3) Calculation of the correlation matrix for all pairs of channels or nodes. (4) Thresholding of the correlation matrix into a binary adjacency matrix. (5) Visualization of the binary adjacency matrix as a graph.

doi:10.1371/journal.pone.0045771.g001

modified Beer-Lambert law with a differential path length factor of 6 for each wavelength [38,39]. Note that the sum of oxy-Hb and deoxy-Hb is defined as total-Hb. In this study, we chose oxy-Hb signal to perform comprehensive network analysis and evaluate reproducibility of network metrics across subjects and over time. Meantime, as a complement to hemoglobin contrasts, deoxy-Hb and total-Hb were also chosen to investigate whether they have similar network properties to those of oxy-Hb. The sampling rate for the optical signal was set to 25 Hz, which resulted in 12000 sample points from each 8 min dataset that could be used for further analysis.

Construction of fNIRS-based Brain Networks

Nodes and edges are two fundamental elements of a network. In this study, the nodes were defined naturally as measurement channels and edges were defined as functional connectivity between nodes. Functional connectivity was quantified by computing Pearson correlation coefficients for the time series between pairs of nodes. Therefore, for each participant we obtained an $N \times N$ correlation matrix ($N=46$, the number of fNIRS channels). We then averaged all of the individual correlation matrices and converted the resultant population-based mean correlation matrix into a binary graph (i.e., adjacency matrix) by applying a predefined correlation threshold, T , such that edges with **absolute connectivity strengths**, $r(i,j)$, larger than T were set to 1 and all others were set to 0:

$$e_{ij} = \begin{cases} 1 & \text{if } |r(i,j)| \geq T \\ 0 & \text{otherwise} \end{cases} \quad (1)$$

In this study, the correlation threshold T was determined in terms of sparsity (S) measure that is defined as the number of actual edges in a network divided by the maximum possible number of edges in a network. Because there is currently limited knowledge about R-fNIRS-based network topology, in this study, we thresholded the mean correlation matrix over the full sparsity range of $0 < S < 1$ (interval = 0.01), which enables us to study network behaviors as a function of sparsity level. Figure 1 illustrates the schematic representation of network constructions using R-fNIRS.

Network Analysis

We analyzed the topological properties of the group-level functional brain network derived from R-fNIRS data in terms of 8 global and 3 local nodal network metrics. The eight global network metrics included small-world properties (clustering coefficient, C_p , characteristic path length, L_p , normalized clustering coefficient, γ , and normalized characteristic path length, λ), efficiency parameters (global efficiency, E_{glob} , and local efficiency, E_{loc}), hierarchy (β), and modularity (Q). These metrics were used to characterize global topological organization of the whole-brain network. The 3 nodal metrics included nodal degree (k_{nod}), nodal efficiency (E_{nod}), and nodal betweenness (N_{bc}), which were used to examine the regional characteristics of the functional brain network. In the Text S1, we briefly illustrated these metrics with a graph (or network) G consisting of N nodes and K edges. For more details about graph metrics, see [40].

Statistical Analysis

To determine whether a network possesses small-worldness, hierarchy and modularity, the small-world parameters C_p and L_p , network efficiency E_{glob} and E_{loc} , hierarchy β and modularity Q were compared to corresponding indices derived from 1000 comparable random null networks. The random networks were generated by preserving the same numbers of nodes and edges and the same degree distribution as the real brain network [41,42]. Then a z-score was calculated as follows: $Z(x) = \frac{x_{real} - \langle x_{rand} \rangle}{std(x_{rand})}$, where x is a network parameter ($C_p, L_p, E_{glob}, E_{loc}, \beta$ or Q) that has a value x_{real} for the real brain network and has a mean $\langle x_{rand} \rangle$ and standard deviation $std(x_{rand})$ for 1000 random networks. A two-tailed significance level of 0.05 (z-score < -1.96 or z-score > 1.96) was used to determine whether the real brain network possesses significantly non-random architecture.

Reproducibility of Network Metrics

To determine the reproducibility of the network characteristics derived from R-fNIRS data, we implemented two additional complementary analyses. First, we divided the 15 participants into two independent subgroups (subgroup 1: $n=7$; subgroup 2: $n=8$). There were no significant differences in age or gender between the two subgroups. Split-half analysis allows us to evaluate the reproducibility of network properties across participants. Second, we divided each participant's whole 8-min dataset into two non-overlapping continuous 4-min sub-datasets (sub-dataset 1 and sub-dataset 2), leaving 6,000 data points for each participant in each sub-dataset. This division allows us to evaluate the reproducibility of network properties over time. For the both reproducibility analyses, functional brain networks were constructed and analyzed separately for each subgroup and each sub-dataset using the procedures as described above.

Results

Small-worldness and Efficiency

Using R-fNIRS data, we obtained a mean population-level correlation matrix (Fig. 1) and investigated its network topological attributes. Before presenting network topological results, we showed the distribution of correlation values within the matrix (Fig. 2A) and plotted the connectivity pattern for the topmost ranked 10% connections (correlation values > 0.67) in anatomical space (Fig. 2B). We found that the correlation values showed an approximately normal distribution (mean = 0.54) and the connections were positioned in a structured manner. For subsequent network analysis, the mean correlation matrix was thresholded into a series of brain networks over the whole sparsity range of $0 < S < 1$. Figure 3 shows the profiles of small-world parameters (clustering coefficient and characteristic path length) and network efficiencies (local efficiency and global efficiency) as functions of sparsity threshold. For both the real brain network and random networks, we found that the clustering coefficients (C_p^{real} and C_p^{rand}) increased with sparsity threshold and that the characteristic path lengths (L_p^{real} and L_p^{rand}) decreased monotonically with sparsity threshold (Fig. 3A and B). When compared to matched random networks, the clustering coefficients C_p^{real} of the real brain network